Performance Prediction of Turbomachinery Cascades as Affected by Upstream Turbulence

Umit Kus, Jacques Chauvin

Classification
Physics Abstracts
47.80V — 47.32Ff — 47.40Hg

Performance Prediction of Turbomachinery Cascades as Affected by Upstream Turbulence

Umit Kus and Jacques Chauvin

Lab. d'Energétique et de Mécanique des Fluides Interne, URA CNRS 1504, Univ. Paris VI, CNAM, ENSAM Orsay, France

(Received 21 September 1994, accepted 3 July 1995)

Abstract. — The problem of predicting the quasi-2D performance of turbomachinery blade cascades is presently the object of a considerable amount of research, especially for off-design conditions where separation is occurring frequently. This interest is particularly vivid for the case of multi-blade row axial machines, where upstream wakes affect the blade operation, especially the transition and separation processes. This paper presents a fast modelling method, based on a strong coupling between a potential flow calculation and an integral approach for the boundary layer and separation regions, taking into account the main effects of the upstream wakes. Comparisons of global (loss and deviation) and local performance (local boundary layer parameters including the transition and separation regions) with and without upstream wakes effects are presented as well as with the scarce -and not always reliable- experimental data available.

Nomenclature

c	chord length	L	Truckenbrodt form factor
C_D	dissipation factor	L_λ	characteristic length for transition
C_f	skin friction coefficient	L_T	total transition length
f	flow integral quantity	$L_{T_{min}}$	minimum transition length
g	spot production function	n	turbulent spot production rate
H_{12}	shape factor $= (\delta_1/\delta_2)$	P	static pressure
H_{32}	shape factor $= (\delta_3/\delta_2)$	P_t	total pressure
i	incidence angle	Re	Reynolds number
K	acceleration parameter	s	arc length in stream wise direction
Tu	turbulence intensity in percent $Tu = \frac{\sqrt{\overline{u'^2}}}{U}$	U	incident velocity
		u'	fluctuation term in velocity
x	surface co-ordinate in stream wise direction	X	energy related quantity (Eq. 4)

Greek Symbols

α	angle of attack
β	flow angle from axial direction
δ_1	displacement thickness
δ_2	momentum thickness
δ_3	energy thickness
γ	intermittency factor or stagger angle
$\overline{\Lambda}_2$	averaged Pohlhausen parameter
λ_θ	pressure gradient parameter
ν	kinematic viscosity
$\overline{\omega}$	loss coefficient
ω	wake passing frequency
ω_r	reduced frequency
σ	solidity or/and Emmon's spot propagation parameter
θ	turning angle
τ	wake passing period

Subscripts

cr	critical
e	external
E	end of transition
I	at instability
lam	laminar
n	neutral (Schlichting's) or quantity related to the normal modes of transition
sep	at separation
t, T	at transition (onset)
trans	transitional
turb	turbulent
w	quantity related to wake-induced transition
x	surface co-ordinate in stream wise direction
0	surface value
1	cascade inlet
2	cascade outlet

Modifying marks

$-$	ensemble-averaged quantity
$\sim$	time-averaged quantity

Abbreviations

DCA	Double Circular Arc
LE	Leading Edge
PS	Pressure Side
SS	Suction Side
TE	Trailing Edge

Introduction

The generalized radial equilibrium approach remains one of the tools currently in use for the calculation of axial flow turbomachines performance. In that context, the problem of predicting correctly the quasi 2D performance of turbomachinery blade cascade has to be addressed especially for off-design condition where separation is occurring frequently. As most of axial turbomachines are multi-blade row, the effect of upstream wake on the performance must be taken into account at least approximately.

We describe below a fast (75 s per data point on a PC 486 DX2 66) approach for modelling this type of flow. It resorts on a strong coupling between an inviscid potential flow calculation and an integral boundary layer approach, which restores the mean features of the flow such as losses and turning, boundary layer and separation region characteristics for the laminar, transitional, turbulent and separated flows including the effect of the wakes of the upstream blade-row.

After a short description of the method, its partial validation is described. The method is then used to predict the effect of free-stream and upstream-wake turbulence on the performance of typical compressor and turbine cases.

1. Flow Model

1.1. General Layout. — The viscous-inviscid interaction method used in the present work was designed to model the phenomena typically occuring in a subsonic, incompressible, steady flow in cascades of airfoils. The inviscid flow is simulated by a singularity method using the potential flow equations in two versions, one compressible and one incompressible used in this study. The incompressible potential equations are solved using the incompressible panel method developed by Van Den Braembussche [1], based on the theory of Martensen [2]. The code of Van Den Braembussche exhibits a remarkable computational stability and allows the implementation of the free streamline model for separation in a straightforward way [3]. Between 30 and 60 panels are used, more closely spaced near the leading and trailing edges.

The viscous solver is built up from integral models of the boundary layer development. These include:

- the laminar boundary layer development from the leading edge stagnation point up to the transition onset,
- the transitional boundary layer development (natural, by-pass, periodic unsteady or by the formation of a laminar separation bubble which may reattach after transition ends or burst into a separated flow region),
- the attached turbulent boundary layer development, until its separation if it occurs,
- the separated flow region which extends until the trailing edge, if it exists.

1.2. Boundary Layer Calculations

Laminar Region

The laminar boundary layer is computed by solving the Von Karman integral incompressible boundary layer equations [4].

$$\mathrm{d}\left(\delta_2 U_e^2\right) + \delta_1 U_e \mathrm{d}U_e = C_f \frac{U_e^2}{2}\,\mathrm{d}s \tag{1}$$

$$\mathrm{d}\left(\frac{\delta_3 U_e^3}{2}\right) = C_D \frac{U_e^3}{2}\,\mathrm{d}s \tag{2}$$

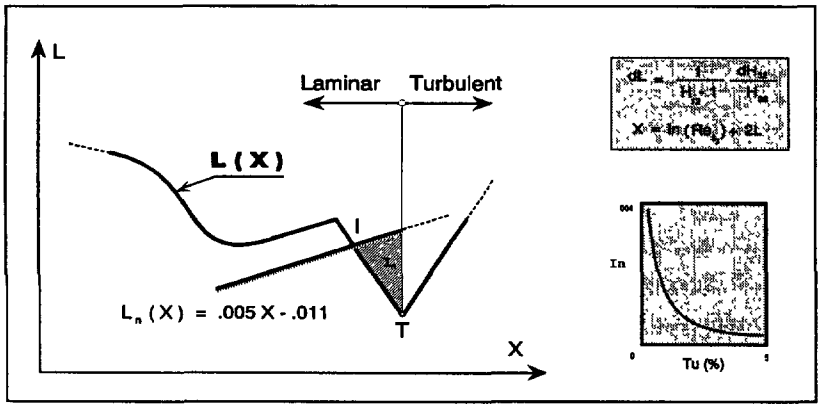

Fig. 1. — Schematic representation of Le Foll's $L(X)$ plane.

These equations are solved using the integral method developed by Papailiou [5] and Huo [6] based on the theory formulated by Le Foll [7]. In this theory, Le Foll transforms the above equations using the Truckenbrodt form factor (L) which is defined by a total differential as a function of boundary layer shape factors, namely:

$$\mathrm{d}L = \frac{1}{H_{12} - 1} \frac{\mathrm{d}H_{32}}{H_{32}} \tag{3}$$

and its linear combination with the energy thickness Reynolds number logarithm (X):

$$X = \ln(Re_{\delta_3}) + 2L \tag{4}$$

Le Foll presented all the boundary layers on a plane using those two parameters (L, X). With L as ordinate and X as abscissa, he obtained a plane where each point represents one station of the boundary layer development (see Fig. 1, a schematic representation of Le Foll's L, X image plane). If the points from station to station are traced, one obtains a curve $L(X)$, which represents the boundary layer development. Since L is calibrated so that $L = 0$ at separation, therefore all the points on this plane lying above the abscissa ($L = 0$) represent all the unseparated boundary layers. The boundary layer computations start from the stagnation point. Papailiou [8] has determined a value of L at this point ($L = 0.04362$).

Finally, the Falkner-Skan boundary layer profiles [4] are used for the closure of the integral equations.

Transition Region

The treatment of this region is one of the main topics of this paper and it is dealt with in detail in the next Section.

Turbulent Region

The turbulent boundary layer development is simulated using the integral incompressible boundary layer equations where the normal fluctuation terms are taken into account. These equations are solved using a method analogous to the one used for computing the laminar

boundary layer [5, 6]. The closure of the integral equations is obtained using a family of turbulent boundary layer velocity profiles, proposed by Le Foll which give results quite similar to the Coles [9] family.

Turbulent Separation

When turbulent separation is reached, and in order to avoid complex and lengthy viscous-inviscid interaction methods, a simple free streamline theory is used. This type of model has been used both for the external flow applications [10], and for the cascades by Janssens and Hirsch [11], Geller [12]. After testing several models [13–15], the most suitable is that of Jacob. It consists in simulating the separated zone as an isobaric streamline, emanating from the separation point which is evaluated iteratively. A standard source distribution is made on the profile surface downstream of the separation point. Its intensity is imposed in such way as to have a constant pressure at the borderline of the separation region.

2. Transition

The laminar - turbulent transition in gas turbine engines develop over a major part of the blade surfaces, so it is important to take into account a procedure modelling the transitional flow regions.

In the present study, four types of transition are considered. The first and most known is natural transition. This type of transition begins with a weak instability in the laminar boundary layer as described first by Tollmien-Schlichting [4] and proceeds through various stages of amplified instability to the fully turbulent flow. The second type, frequently called "by-pass" transition following Morkovin [16], is caused by large disturbances in the external flow (such as free-stream turbulence) and completely bypasses the Tollmien-Schlichting mode of instability. This is the common type of transition in gas turbines due most of the time the existence of high level free-stream turbulence in those environments. The third type is separated flow transition. This type of transition occurs in a separated laminar boundary layer and may or may not involve the Tollmien-Schlichting mode of instability. This type of transition also occurs in both compressor and turbines of gas turbine engines. The fourth type is "wake-induced transition" following Mayle & Dullenkopf [17]. This type of transition is caused by the periodic passing of wakes from upstream blade rows or obstructions. The periodic passing of a shock wave can also produce this type of transition.

2.1. NATURAL AND/OR BY-PASS TRANSITION. — In the present study, for the two first type, the prediction of transitional flow is carried out in two steps: transition onset and transition length. First the start of transition is predicted by using several transition onset criteria. Then Emmons' Intermittency concept is used in order to predict the transitional values of boundary layer integral parameters such as thicknesses and shape factors. Several criteria are used for predicting the intermittency distribution which corresponds to the transition length.

Emmons [18] provided an expression for the fraction of time during which the flow at any location on the surface is turbulent, which is called "Intermittency γ". Since the flow in the transition region is part of the time laminar and part of the time turbulent in the relative proportion of $(1-\gamma)/\gamma$, Emmons presumed that the time-averaged flow at any stream wise position may be considered as a superposition of the two, according to:

$$f = (1-\gamma) f_{\text{lam}} + \gamma\, f_{\text{turb}} \tag{5}$$

Table I. — *Summary of the transition criteria.*

Authors	Remarks
Michel (1952)	Onset, Experimental data and experimental investigations, flat pate or pressure gradient $Re_{\delta_2 t} = 1.535 Re_{xT}^{0.444}$, x_T. from the origin of the boundary layer up to x_t, $Re_{\delta_2 t} = 1180$ gives good agreement with data of Schubauer & Skramstad (1948)
Granville [Cousteix (1989)]	Onset, Experimental data with theory of stability on flat plate for Tu ($\leq$ 0 1) and pressure gradient (0,+,-), $Re_{\delta_2 t} = f\left[(Re_{\delta_2 ins}(H_{12}), \bar{\Lambda}_2)\right]$
Van Driest & Blumer (1963)	Onset, Experimental data and theoretical studies on flat plate and bodies of revolution, semi-empirical expression for $Re_{\delta_2 t} = f(\lambda_\theta, Tu)$ for 0.0<Tu<3 0
Wilkinson [Papailiou (1969)]	Onset, Theory of stability, flat plate, $Re_{\delta_2 t} = f(Tu)$ and implicitly pressure gradient (-,+,0) with (0 0<Tu<5 0)
Abu Ghannam & Shaw (1980)	Onset, Experimental data and experimental investigations, incomp flow, flat plate, Tollmien-Schlichting type of instabilities, semi empirical expression of $Re_{\delta_2 t} = f(\lambda_\theta, Tu)$ for the range of pressure gradients (0,-,+) and (0 3<Tu<5 0)
Arnal et al (1984)	Onset, Extension of Granville, flat plate, bodies of revolution and swept wing with infinite span, $Re_{\delta_2 t} = f(Re_{\delta_2 ins}, \bar{\Lambda}_2, Tu)$ for pressure gradient (0,+,-) and (0 0<Tu≤1 0)
Dhawan & Narasimha (1958)	Length, Experiments on flat plate, 2D, incomp. flow, pressure grad (0), investigations on spot formation Natural transition, $\gamma = f(x_t, L_\lambda)$, semi-empirical expressions required for L_λ Transition ends with γ = 0.99
Abu Ghannam & Shaw (1980)	Length, Experiments and experimental data on flat plate, 2D, incomp. flow, pressure grad (0,+,-), Tu level Natural transition, $\gamma = f(Re_{xt}, Re_{xE})$, semi empirical expression for the prediction of transition end $Re_{xE} = f(Re_{xt})$ for pressure grad (0) and $Re_{\delta_2 E} = f(Re_{L_\lambda}, \lambda_\theta)$ for pressure grad (+,-).
Arnal et al (1980)	Length, Experiments on flat plate and bodies of revolution, 2D, incomp flow, pressure gradient (0,+) Natural transition, $\gamma = f(\delta_2/\delta_{2t})$ transition ends with γ = 0 99
Mayle (1991)	Length, Extension of Dhawan & Narasimha, 2D, incomp flow, pressure gradients (0,+,-), various Tu level Natural or/and Bypass transition, $\gamma = f(\sigma, n, x_t, Tu, K_t)$, transition ends with γ =0 99

where f is a boundary layer flow integral parameter, $f_{\rm lam}$ is its local laminar value, and $f_{\rm turb}$ is its local fully turbulent value. Using this concept, the boundary layer integral parameters through transition were obtained such as:

$$\delta_{1\rm trans} = (1-\gamma)\delta_{1\rm lam} + \gamma\ \delta_{1\rm turb}$$

$$H_{12\rm trans} = (1-\gamma)H_{12\rm lam} + \gamma\ H_{12\rm turb}$$

$$C_{f_{\rm trans}} = (1-\gamma)C_{f_{\rm lam}} + \gamma\ C_{f_{\rm turb}}$$

For natural and/or by-pass type of transition, several criteria concerning the onset and length of transition region were tested. These are Michel [19], Abu Ghannam & Shaw [20], Wilkinson (Papailiou [5]), Van Driest & Blumer [21], Granville (Cousteix [22], Arnal *et al.* [23] for the transition onset prediction and Arnal *et al.* [24], Abu Ghannam & Shaw [20], an advanced modified form of Dhawan & Narasimha [25], Mayle [26] for the transition length prediction. Table I sum up the main characteristics of various criteria, for both onset and length of transition.

A preliminary study, not reported here, lead us to keep for comparison (with experimental data and between themselves) two transition onset (Arnal *et al.* and Wilkinson's) and three

transition length (Arnal *et al.* Dhawan & Narasimha and Mayle) criteria which have been discussed by the present authors in an ASME paper [27].

In this study, we have chosen to discuss only, Wilkinson's onset and Dhawan & Narasimha's length criteria.

Onset Criterion

Wilkinson's criterion has been presented by Papailiou [4] using Le Foll's (L, X) plane where Schlichting's neutral stability curve

$$L_{\mathrm{n}}(X) = 0.005X - 0.011 \tag{6}$$

and the characteristic curve $L(X)$ of any laminar boundary layer can be represented.

Once $L(X)$ curve is below the $L_{\mathrm{n}}(X)$ curve, the laminar boundary layer becomes unstable and transition will take place at a position depending on the turbulence level. Here, Wilkinson postulated a point transition where laminar boundary layer stops and the turbulent calculation begins.

The sketch of this situation is given in Figure 1 (after Huo [6]), where instability begins at point I, which is the point of the intersection of $L(X)$ and $L_{\mathrm{n}}(X)$. Transition will take place if the integral In (the shadowed area below the $L_{\mathrm{n}}(X)$ curve):

$$\mathrm{In} = \int_{X_{\mathrm{I}}}^{X_{\mathrm{T}}} (L_{\mathrm{n}} - L)\, \mathrm{d}X \tag{7}$$

attains a value which is explicitly a function of turbulence level (also see Fig. 1)

$$\mathrm{In} = \mathrm{In}\ (Tu) \tag{8}$$

but also implicitly of pressure gradient because of the past flow history taken into account by two curves $L(X)$ and $L_{\mathrm{n}}(X)$.

Length Criterion

Dhawan & Narasimha [25] expressed the (universal) intermittency distribution through natural transition by:

$$\gamma(x) = 1 - \exp\left[-0.412\left(\frac{x - x_{\mathrm{t}}}{L_\lambda}\right)^2\right] \tag{9}$$

where, x is the distance along the surface, $x_{\mathrm{t}} = x_{\gamma=0}$ is the location of natural transition which is calculated by a transition onset criterion, here is that of Wilkinson, and L_λ is the characteristic length for transition. To consider also by-pass type of transition, a relation must be found between L_λ and the most influent parameters acting on transition such as pressure gradient and free-stream turbulence level. This is made from the review of literature which follows.

Recently Gostelow *et al.* [28] proposed an extended correlation evaluated from Walker's [29] minimum transition length model. The correlation is:

$$\frac{L_{\mathrm{T}}}{L_{\mathrm{T}_{\mathrm{min}}}} = 9.412 \exp[-3.12\ \lambda_{\theta \mathrm{t}}\ \ln(Tu) + 33.692\ \lambda_{\theta \mathrm{t}} + 0.248\ \ln(Tu)] \tag{10}$$

where $\lambda_{\theta t}$ is the pressure gradient parameter at the start of transition, Tu is turbulence level (%), L_T is total transition length which is given by Walker [29] as a function of characteristic length by

$$L_T = 3.36\, L_\lambda \tag{11}$$

and $L_{T_{min}}$ is the predicted minimum transition length.

Walker and Gostelow [30] expressed that the theoretical minimum value is given for $L_{T_{min}}$ that can be given by a relation

$$Re_{l_{T_{min}}} = 2.3\, Re_{\delta_u}{}^{3/2} \tag{12}$$

where δ_{lt} is the displacement thickness at the start of transition.

2.2. Separated Flow Transition. — In the present method, the laminar separation bubbles are computed using the semi-empirical method developed by Roberts [31–33] based on the previous work of Horton [34]. When laminar separation is detected, the location of transition, the boundary layer characteristics at transition and the re-attachment point are determined from the value of δ_2 at separation, the semi-empirical theory of Roberts and the potential flow velocity distribution.

2.3. Wake Induced Transition. — Wakes from upstream blade rows or obstructions are important source of the unsteadiness in flow in gas turbines. This unsteadiness leads to time-averaged losses which can differ appreciably from those measured in isolated blade row (steady flow). For example, Hodson [35] reported that this effect leads to a 50 percent increase in the time-averaged loss of his rotor. It has been shown by several authors that the transition, as a result of the unsteady passing of wakes from the upstream airfoils, is unsteady and cannot be predicted using steady flow boundary layer analysis. Several investigators found also that the wakes directly influenced the onset of transition. This type of transition is called "wake-induced transition". In order to simulate the unsteady effects of passing wakes, in the semi-steady form, Pfeil and Herbst's approach [36] and Mayle and Dullenkopf's theory [17, 26] are used in the present work.

Pfeil and Herbst [36] and later Pfeil *et al.* [37] showed that the wakes caused the boundary layer to become turbulent during their impingement on the surface. This formed wake-induced transition zones, which propagated downstream at a velocity less than the wake passing velocity. These authors implied that the time-averaged condition of the boundary layer may be obtained from:

$$\overline{f} = (1 - \tilde{\gamma})\mathrm{f_{lam}} + \tilde{\gamma}\ \mathrm{f_{turb}} \tag{13}$$

which is similar to equation 5 except that $\tilde{\gamma}$ is now the time-averaged intermittency. Pfeil and Herbst discovered regions of natural transition occurring between those induced by the wake. This implies that multiple modes of transition can occur independently of one another on the same surface at the same instant. The situation is shown in Figure 2 [26] where the normal-mode transition is considered to originate at x_{tn} (for example natural transition), while the wake induced transition is now considered to originate at x_{tw}. At the instant depicted, the boundary layer, which is first laminar (to the left of x_{tw}), becomes turbulent (at x_{tw}), then laminar (between x_{tw} and x_{tn}) and turbulent again.

As for Mayle and Dullenkopf [17,26], they proposed a model based on Emmons [18] turbulent spot theory that considered a coalescence of turbulent spots into turbulent "strips" which propagated and grew along the surface within the laminar boundary layer. They formulated

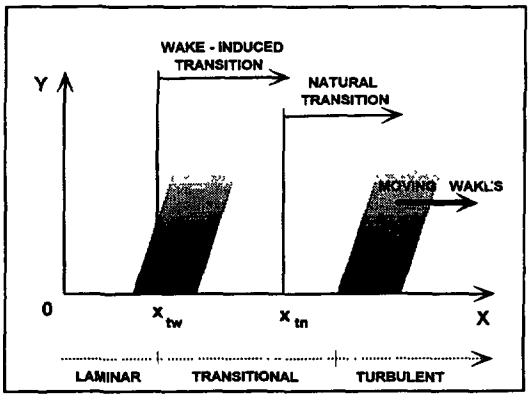

Fig. 2. — Combined wake-induced and natural transition on a surface [26].

the idea that the wake is a production source of turbulent spots so dense that the spots immediately form a turbulent "strip" and once the turbulent strip is formed by the wake, its propagation and growth are independent of the wake propagation in the outside flow (see Fig. 3 of Mayle & Dullenkopf [26]). As a result, their theory predicts a wake-induced intermittency distribution without any need to calculate the wake position after the impingement which allows to use the time-averaged flow for calculating the boundary layer characteristics.

Their extension of Emmons' theory consists of two main points. First, they considered that transition can occur in multiple modes such that two or more types of transition can be occurring simultaneously as shown in Figure 2. Second, they considered a production of turbulent spots from two types of sources. In particular, the turbulent spots are produced both normally (through a normal "steady" mode) and by the periodic passing of wakes imbedded in the free-stream (wake-induced transition). They assumed that the production functions from each source are independent of one another and that the function associated with each source could be linearly superposed such that:

$$g = g_{\mathrm{n}} + g_{\mathrm{w}} \tag{14}$$

where g_{n} and g_{w} are the individual production functions associated with natural and wake-induced transition, respectively. So they proposed the time-averaged intermittency $\tilde{\gamma}(x)$ such as:

$$\tilde{\gamma}(x) = 1 - [1 - \gamma_{\mathrm{n}}(x)][1 - \tilde{\gamma}_{\mathrm{w}}(x)] \tag{15}$$

where γ_{n} and $\tilde{\gamma}_{\mathrm{w}}$ are the intermittency functions associated with the individual source functions for natural and wake-induced transition and the tilt refers to a time averaged quantity over the wake passing period.

The intermittency γ_{n} can be chosen such as one given by equation 9 for instance, where (x_{t}) the onset of transition and (L_{λ}) characteristic length for transition are given by the expressions for the appropriate normal mode of transition (natural or by-pass).

For the time averaged wake induced intermittency $\tilde{\gamma}_w$, Mayle & Dullenkopf [26] uses an expression of the form:

$$\tilde{\gamma}_w(x) = 1 - \exp\left[-1.9\left(\frac{x - x_{tw}}{U\tau}\right)\right] \tag{16}$$

where, U is the airfoil's time averaged (or steady) incident velocity and τ is the wake-passing period.

Later, Hodson *et al.* [38] showed that this correlation defines well unsteady transition in particular when the dependence on wake-width is weak.

Expressing τ in terms of the wake-passing frequency, ω, and introducing a chord length, c, Mayle & Dullenkopf [26] obtained an equation incorporating the reduced frequency ω_r:

$$\tilde{\gamma}_w(x) = 1 - \exp\left[-0.302\,\omega_r\left(\frac{x - x_{tw}}{c}\right)\right] \tag{17}$$

where

$$\omega_r = \frac{\omega c}{U} \tag{18}$$

From this, it can be deduced that the time-averaged wake-induced intermittency depends only on the reduced frequency (ω_r) which is an input for the problem, and the beginning of transition x_{tw} which must be evaluated.

The evaluation of this point is based on the following observations. First, as discussed above, the unsteadiness of the external flow due to the wakes, is of secondary importance on the development of the boundary layer which can be calculated using a time-averaged or the steady flow at least for the range of reduced frequencies encountered in most of the turbomachinery (Obremski & Fejer [39], Pfeil & Herbst [36]). Secondly, the effect of the turbulence level in the external flow on the beginning of transition for the steady flow is important (Abu Ghannam & Shaw [20], Schubauer & Skramstad [40], Hodson [41], Gostelow and Walker [42], Mayle [43]).

From those two points it can be supposed that, in fact, the effect of the wake on the boundary layer is essentially due to the high-local instantaneous level of turbulence acting as a switch to generate turbulent spots as ascertained by Hodson [41]. Consequently, in agreement with Pfeil and Herbst [36], the beginning of transition due to the wakes is calculated by the steady flow approach mentioned above using a very high level of turbulence typically 5 to 10%. The first value is used in our calculations.

3. Performance Evaluation

3.1. Scope of the Evaluation. — The coupling method described above allows to obtain the local characteristics of the boundary layer as well as the global performance.

The local performance are the local boundary layer thicknesses, shape factors, the existence, position and length of laminar separation bubbles when appropriate, beginning of transition, length of transition region, the turbulent separation point when existing. The global performance are the exit angle, (β_2), and the loss coefficient, $\overline{\omega}$, which is defined as:

$$\overline{\omega} = \frac{P_{t_1} - P_{t_2}}{P_{t_1} - P_i} \tag{19}$$

where $i = 1$ is for compressor cascades and $i = 2$ is for turbine cascades. The exit angle is obtained from the calculated outlet flow angle at the end of the convergence process involving

both potential and the boundary layer type of calculation. The loss coefficient is obtained by calculating the mass-weighted averaged total pressure at the cascade exit-plane, the reduction of the total pressure being due to the boundary layer and the separation region. For the latter, the boundary layer computation stops at the separation point. The value of the displacement thickness at the trailing edge is known as it is equal to the dividing streamline height from the blade surface, while the momentum thickness at trailing edge is obtained from the shape factor H_{12} which is calculated using an empirical model based on NACA results (NACA TN 3916):

$$H_{12} = 37.82\, x_{sep}^2 - 73.83\, x_{sep} + 38.02 \qquad 0.5 < x_{sep} < 1.0 \tag{20}$$

In this second order polynomial function x_{sep} represents the separation point, in percent chord. The above expression gives a good approximation compared to that of Simpson [44] and Heillman [45].

If a large body of cascade global performance is available in the literature both for compressors and turbines (for instance, NACA TN 3916 and NACA TN 3802), there is a dramatic lack of reliable experimental data on local performance.

Comparison of global performance calculation with the experimental data, selected from some 250 data points treated (Yazigi, [46]), is given for compressor (NACA 65) and turbine (NACA A3K7) cascades.

For the NACA 65 compressor cascade the classical data of Herrig *et al.* [47] has been used. The measurements have been taken in a cascade tunnel where two dimensionality and periodicity could be achieved by boundary layer suction on the walls. Due to the tunnel configuration, the tests are carried out for discrete air inlet angles β_1 and the angle of attack α is changed by varying the blade stagger angle γ. The test Mach number is about 0.1 and the Reynolds number, based on the chord and the inlet velocity, is about 0.25×10^6. For the NACA A3K7 turbine cascade the data of Dunavant and Erwin [48] has been used. The test Mach number is about 0.1 and the Reynolds number, based on the chord and the inlet velocity, is about 0.35×10^6.

The accuracy of NACA data is estimated to be $\pm 1°$ for the exit angle and ± 0.01 for the losses, except for the separated cases where the inaccuracies are higher. The results of computation is considered as correct, when the difference between calculated and measured data falls within those brackets.

The measurement on a compressor blade in cascade by Deutsch and Zierke [49–52] is used for comparison of local and global performance. In the tests, a periodic, two-dimensional flow field has been achieved, except apparently in the highest incidence separated case, at a chord Reynolds number of 0.5×10^6. Measurements are taken at the incidence angles of $i = 5.0$, -1.5 and -8.5 degrees on a highly loaded, five - double circular arc compressor blade cascade. Deutsch and Zierke measured both the global performance using five-hole probes and the local boundary layer and near wake parameters using a single component LDV.

Using those data, we considered first, the performance evaluation without wake effects. We first compared measured and calculated data without taking into account wake-induced type of transition. For the latter, some parametric studies have been carried out considering both the free stream and wake turbulence effect on the performance.

Table II. — *Comparison on local performance basis without wake.*

	i = -1.5 °		i = -8.5 °		i = 5.0 °	
	SS (x/c)%	PS (x/c)%	SS (x/c)%	PS (x/c)%	SS (x/c)%	PS (x/c)%
FLOW MODEL	A 31 / 39	9 / 21	42 / 50	8 / 19	-	-
	B 38 / 39	20 / 21	49 / 50	17 / 19	-	-
	C 84	-	97	-	-	-
	D -	-	-	-	14 / 46	27 / 82
	E -	-	-	-	60	-
DCA DATA	A 3 / 9	14±6 / 38±5	35 / 60	>4 / <10	<3 / 13	-
	B <9 / 9	<38±5 / <61	55 / 60	>4 / <10	<13 / 13	-
	C ~70 → 86	-	~92	-	66±4	-
	D -	-	-	-	-	64±4 /
	E -	-	-	-	-	-

3.2. No-Wake Performance Evaluation

Local Performance Evaluation

Deutsch & Zierke's DCA test data is used for comparison on local performance basis. Table II represents this comparison by means of the main boundary layer features, i.e.:

A the laminar separation bubble onset/end

B the onset/end of transition in the bubble

C the turbulent separation point (if it exists) in case of bubble transition

D the natural and/or bypass transition onset/end

E the turbulent separation point for the normal mode transition

$i = -1.5°$: on the suction and pressure sides, due to the calculated detection of laminar separation bubbles, the normal mode (natural and/or bypass type) transition criteria are not applicable. On the suction surface, the laminar separation bubble is predicted using Roberts' separated flow transition approach, to occur between 31-39% chord, but the test data indicates this bubble earlier (3-9%) near the leading edge. A turbulent separation is detected at 84% chord by the calculations and between 70 to 86% chord by the tests. For the pressure surface, the laminar separation bubble is detected between 9-21% by the calculation which falls within the large bracket of the experimental data. There is no turbulent separation detected for both calculated and measured data for this surface. The test results also indicate that separated flow transition in the bubble is not complete and extent even after the bubble re-attachment.

$i = -8.5°$: for the suction surface a laminar separation bubble is detected somewhat later and shorter than the test data results. For both calculated and measured data, transition is of the separated flow type and its length is small with respect to the bubble length and the turbulent separation takes place after 90% chord. For the pressure side, both calculated and measured data indicate that the bubble onset takes place in the vicinity of the leading edge, transition is short and there is no turbulent separation.

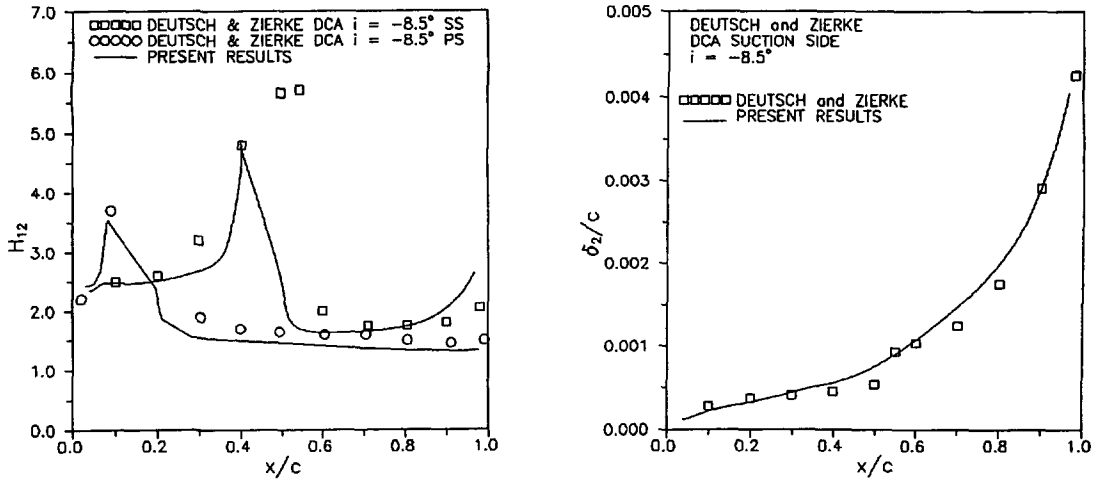

Fig. 3. — Comparison of boundary layer integral parameters.

$i = 5.0°$: for the suction surface, the calculation predicts a normal mode of transition beginning at 14% and ending at 46% chord. The turbulent separation is predicted at 60% chord. While, the test results indicate the existence of a laminar separation bubble which is in vicinity of the leading edge region and a turbulent separation at nearly 66% as well. The pressure side for this incidence is the only one for which there is clearly no bubble detected experimentally. The measurement indicates a very late (at 64%) and uncompleted transition, while the onset criterion indicates the beginning of transition at 27% and the length criterion gives the end of transition at 82% chord.

The flow method described above is also able to predict the local boundary layer thicknesses and shape factors. This is typified by Figure 3 corresponding to the case of $-8.5°$ incidence angle of DCA cascade. The agreement is very good for the shape factor on the pressure side and for the momentum thickness on the suction side. The shape factor evaluation on the suction side is somewhat underestimated in the separation bubble region. For the cases where the main features are not well predicted, it is evident that there are also discrepancies on the local integral boundary layer parameters.

For the cases where laminar separation bubbles have been identified experimentally, their position (onset and length) is correctly predicted within the expected accuracy on the pressure side. For the suction side, the tendency of the calculation is to give a later onset and a nearly correct length. We believe that this is due to the difficulties of the potential flow method to deal with very thin leading edges.

Not withstanding our efforts, we are still unable to explain the failure of our method to predict the boundary layer behaviour for the incidence angle $i = 5.0°$, both suction and pressure sides. Nevertheless, we believe that the free stream turbulence level, used in the experimental investigation for this particular incidence angle, which has not been clearly given by the investigators, may cause those types of differences due to its influence on the calculation results in particular for transition region.

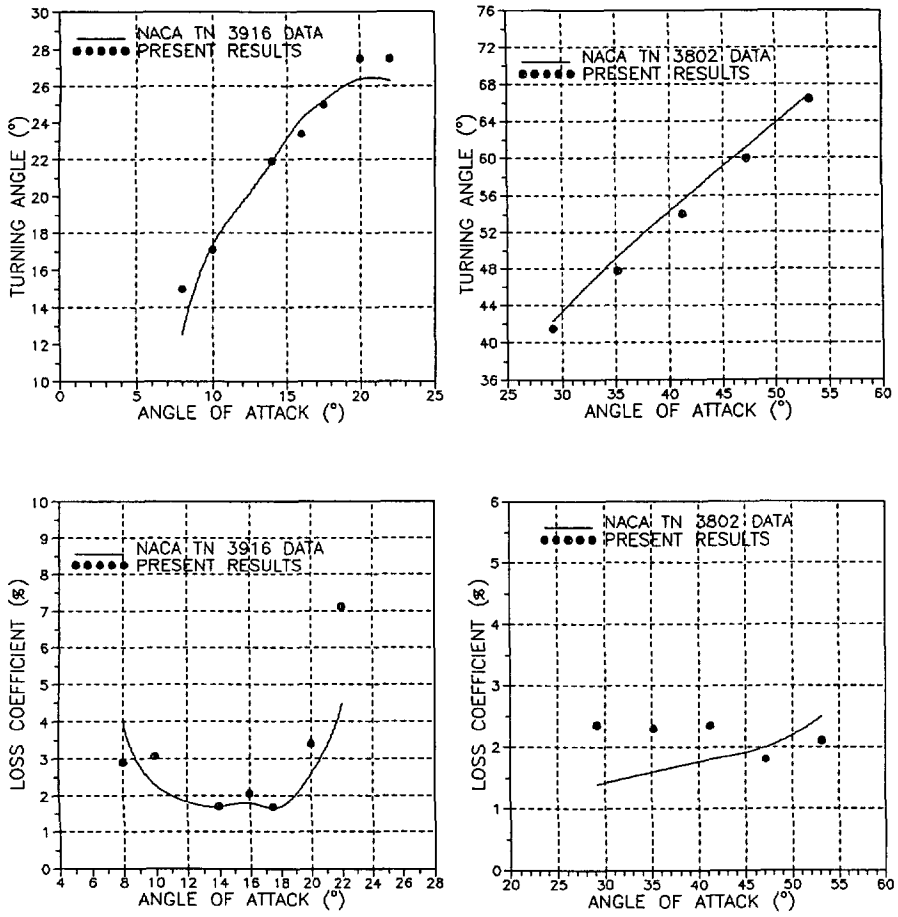

Fig. 4. — Comparison of global performance parameters.

Global Performance Evaluation

On the global performance basis, NACA 65 compressor and NACA A3K7 turbine as well as Deutsch & Zierke's DCA data have been used for comparison. For NACA data, a sketch of the comparison of the turning angle ($\theta = \beta_2 - \beta_1$) and loss coefficient ($\overline{\omega}$) with various angle of attack (α) is presented in Figure 4. A very good agreement is obtained for both the turning angle and the loss coefficient except for the higher angle of attack. For this point, the accuracy of the measurement is questionable, due to the large separation zone existing on the blade surface (compressor case).

Table III represents a typical comparison with NACA and DCA data. NACA compressor data is that of $65 - 18A_{10} - 10$ with $\alpha = 14°$, $\beta_1 = 60°$, $\sigma = 1.0$ and the turning angle θ is 22°. Naca turbine data is that of A_3K_7 with $\alpha = 47.2°$, $\beta_1 = 0°$, $\sigma = 1.5$ and the turning angle θ is 61°.

For Deutsch & Zierke's test data the cases of $i = -1.5°$ and $-8.5°$ correspond to a bubble

Table III. — *Comparison on global performance basis without wake.*

		LOSSES (%)		EXIT ANGLE (°)	
		DATA	AUTHORS	DATA	AUTHORS
D	-8.5°	2 8	3 4	-0 6	3 2
C	-1.5°	9 4	10 4	2 1	3 1
A	5.0°	15 1	14 1	4 0	3 1
NACA 65		1 9	1 7	38 1	38 7
NACA A3K7		2 0	2 8	61 2	60 0

transition. For $i = -1.5°$, the exit angle (calculated: 3.1°, measured: 2.1°) and the losses (calculated 10.4% vs. measured 9.4%) are well predicted within the estimated accuracy. For the case of $i = -8.5°$ the losses are also well predicted (3.4% calculated vs. 2.8% measured), while the exit angle (3.2°) is much larger than that the experimental one (−0.6°). Note that the experimental overturning is a bit surprising as there is no pressure side separation. For the case of $i = 5.0°$, where experimental transition is of separated flow type on the suction surface and natural and uncompleted on the pressure surface, both measured and calculated losses (14.1% calculated vs. 15.1% measured) and exit angles (3.1° calculated vs. 4.0° measured) are satisfactory predicted not withstanding the poor local prediction on the pressure side. This agreement is due, of course, to the fact that it is a case dominated by turbulent separation on the suction surface.

For the NACA data, within the estimated accuracy of measurements, there is a good agreement between calculated and measured values for both losses and exit angles.

3.3. Parametric Study on Turbulence and Wake Effects. — The method having been validated as much as it was possible, it can be used as a tool for comparative parametric studies which can complement the existing experimental information and can provide a data base when no experiments exist. Here, the cases of the effect of free stream turbulence and turbulence due to the upstream wakes are treated.

Effect of Free-Stream Turbulence level

Although the fully laminar and fully turbulent part of the boundary layer are affected by the external turbulence (and this is taken into account in the corresponding models), the main effect is on the transitional region as it affects the point of the beginning of transition, the intermittency factor and therefore the length of transition region.

A parametric study on a range of the free-stream isotropic turbulence from 0.1% up to 7.0%, has been carried out for Deutsch & Zierke DCA compressor cascade ($i = -8.5°$) and for NACA A3K7 turbine cascade ($\alpha = 47.2°$) both used in the previous part.

The results are presented in the form of plots giving the position on pressure and/or suc-

tion surface of the beginning and end of the transition region, the beginning of the laminar separation bubble and of the end of transition in this bubble when appropriate (Fig. 5 and Fig. 6 respectively). Those plots are complemented by plots of the loss coefficient in function of turbulence level (Fig. 7), as well as the evolution of intermittency factor (Fig. 8).

At low turbulence level, there are always laminar separation bubbles which disappear with increasing turbulence level (Fig. 5 and Fig. 6). The level of turbulence at which this appears, being a function of the external velocity distribution, as seen comparing the compressor and turbine cases. The compressor case involves a turbulent separation –on suction side– (Fig. 5a), the point of separation is first moved towards the leading edge when the turbulence level increase, to remain constant above 2.0% of turbulence.

For the compressor case, the loss coefficient (Fig. 7), first increases slightly, then diminishes when a bubble is present, then increases again, but this time sharply, with turbulence in the no-bubble domain to reach an asymptotic value above 5.0% of turbulence. For the turbine case (Fig. 7), there is first a slight increase and then an asymptotic increase with the increase of turbulence level. The increase of turbulence level moves the beginning of transition towards the leading edge as well as the end of transition, while the length of transition first diminishes and then becomes independent of the turbulence level. This asymptotic character can also be seen in the plot of the intermittency factor (Fig. 8).

Effect of Upstream Wake Turbulence

It has been ascertained above that the upstream wake effects were mainly to induce a periodic early start of transition due to the trigger effect of the turbulence in the wake and to add a periodic intermittency, while the unsteadiness of the external flow was of secondary importance, following Mayle's reasoning, although the reduced frequency comes into the picture. The whole problem is to calculate the wake intermittency.

The wake effect is also indicated in Table IV for the cases treated in the preceding paragraph. The calculations are presented for a free-stream turbulence of 0.2% for the compressor case -DCA $i = -8.5°$- (in order to magnify the effect) and of 2.0% for the turbine case -NACA A3K7 $\alpha = 47.2°$- and for a reduced frequency of 10.0, which is typical for turbomachines, for both cases. The main results are presented below:

- The laminar separation bubbles disappear whatever the value of the external flow turbulence.
- The equivalent, steady beginning of transition is moved towards the leading edge.
- For the compressor case (which, without wake effect, corresponds to a transition with bubble on both suction and pressure side), the end of transition moves towards the trailing edge and therefore the length of transition is increased. For the turbine case (and for the compressor case when there is no bubble according to our calculation not reported here), the end of transition moves towards the leading edge and the transition length is reduced. According to our experience, this reduction decreases with the increase of the external turbulence level and disappears when the external level of turbulence is of the order of 5.0%. This particular value comes from the criteria built in the method for the external turbulence level. This behaviour is confirmed by the plot of the intermittency factor (Fig. 9) which gives the resulting intermittency with and without wake effect and by Figure 10, which gives the contribution to the global intermittency ($\gamma_{w,n}$) of the wake intermittency (γ_w) and the normal (natural or by-pass) intermittency (γ_n). This plot shows that the normal intermittency dominates, the influence of the wake intermittency being important only in the early stage of transition. Except near the beginning of transition, the normal mode of transition (without wake effect) still dominates the process. This is confirmed by Mayle's and Hodson's data.
- For the losses: In the compressor case (corresponding to 0.2% free-stream turbulence level),

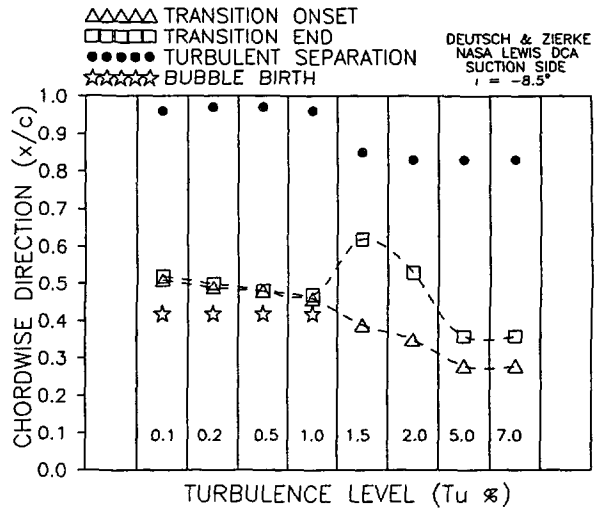

a)

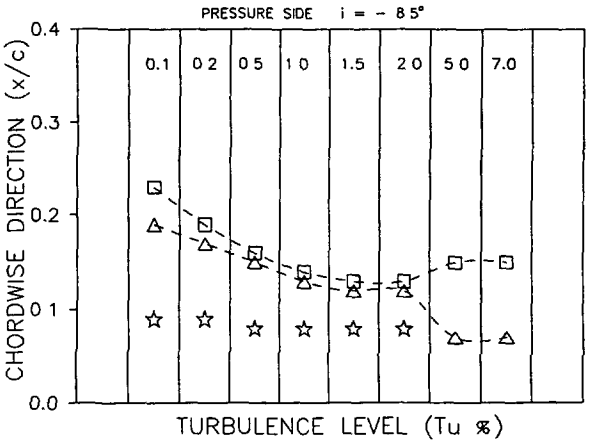

b)

Fig. 5. — a) Boundary layer main features vs. Tu (compressor case SS); b) Boundary layer Main features vs. Tu (compressor case PS).

the losses are considerably increased due to the increase of the length of transition (resulting from to the disappearance of the bubble) and essentially, to the increase of the separated region on suction surface for this particular level of the external turbulence. This effect would be strongly reduced for the high levels of external turbulence.

- For the turbine case (corresponding to 2.0% free-stream turbulence level), the increase of the loss coefficient is moderate. Our experience shows that the large increase in losses, due to the wake, occurs when, without the wake effect, the boundary layer remains transitional at the trailing edge which corresponds to Hodson's [35] case cited above (50 percent increase in the time-averaged loss of the rotor).

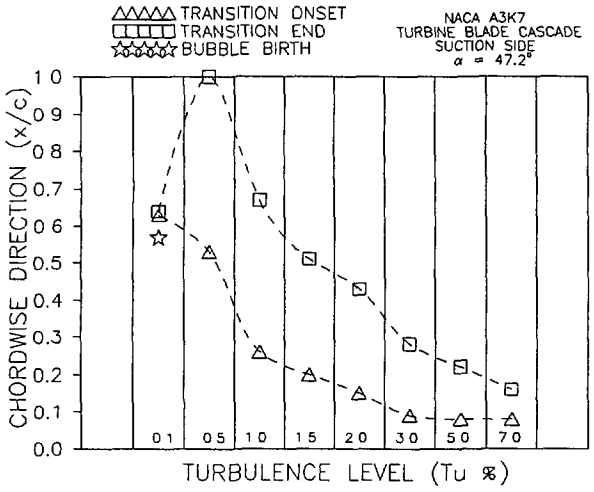

Fig. 6

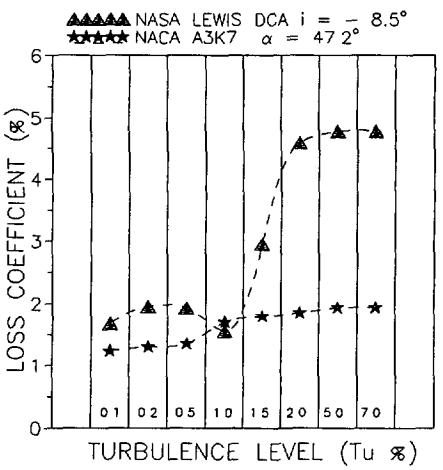

Fig. 7

Fig. 6. — Boundary layer main features vs. Tu (turbine case SS).

Fig. 7. — Loss coefficient vs. Tu.

Table IV. — *Comparison with and without wake.*

FLOW PATTERN		DCA -8.5°				NACA A3K7	
		NO-WAKE		WAKE		NO-WAKE	WAKE
		SS	PS	SS	PS	SS	SS
BUBBLE	(x/c)	0 42	0 08	-	-	-	-
TRANSITION ONSET	(x/c)	0 49	0 17	0 28	0 07	0 15	0 08
TRANSITION END	(x/c)	0 50	0.20	0 80	0.60	0 43	0 28
TRANSITION LENGTH	(x/c)	0 01	0 03	0 52	0 53	0 28	0 20
TURBULENT SEPARATION	(x/c)	0 97	-	0 83	-	-	-
LOSS COEFFICIENT	(%)	1 95		4 78		1 84	1 93

Conclusions

A rapid method of (max. 75 s on PC 486 DX2-66 per data point) computing the global and local performance of axial turbomachinery cascade in incompressible flow has been presented. It has been validated extensively for global performance and compared with success on one of the rare documented cases for local –boundary layer– performance.

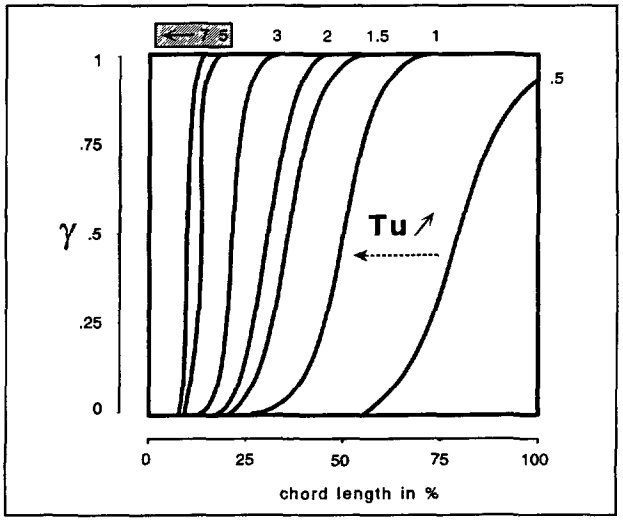

Fig. 8. — Effect of increasing turbulence level on transition region.

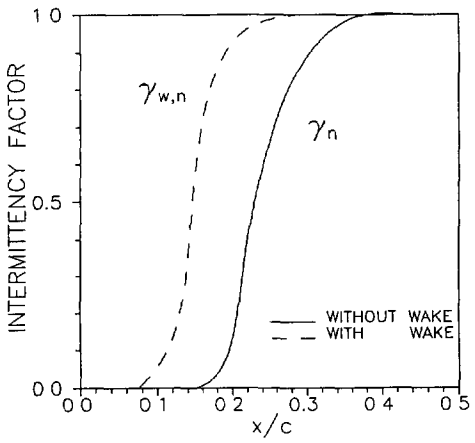

Fig. 9

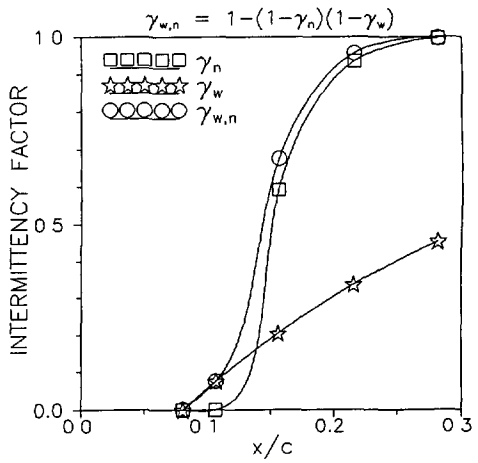

Fig. 10

Fig. 9. — Intermittency factor with and without wake.

Fig. 10. — Contribution to the global intermittency.

The method has been validated extensively for global performance against NACA and DCA data. The local performance has been compared with Deutsch & Zierke's data which was the only detailed information at our disposal. This data is invaluable even if the accuracy of the measurement cannot always be assessed for the boundary layer and the wake characteristics which show sometimes either abnormal evolutions or discrepancies between the different mea-

suring techniques. However, the agreement is good for the case of $i = -8.5°$, for the suction side at $i = 5.0°$ and for the pressure side at $i = -1.5°$. It is to be noted that the test conditions were such as to lead to a separated flow type of transition (due apparently very low level of turbulence intensity - $Tu \approx 0.2\%$) except for the pressure side at $i = 5.0°$.

The method provides a useful tool to estimate the cascade performance for a large range of Reynolds number and turbulence level, and can also be used to detect, in advance of testing, if the experimental condition will show some unwanted character such as bubble transition in the study of the transition region.

A parametric study on the effect of free stream turbulence -without upstream wake effect- and on the effect of upstream wakes –shown to be essentially due to the periodic impact of the wake turbulence– has been presented for two extreme cases one of compressor and one of turbine. The present study showed that the effect of free-stream turbulence level has an asymptotic character above 5.0% for the onset and length of transition region and this is so whatever the type of transition. Additionally, the wake-induced intermittency dominates transition process only in its early stages. For the rest of the process, the normal mode of intermittency dominates completely the phenomenon.

Acknowledgments

This work was supported in part by DRET (Direction de Recherches & Etudes Techniques) under the contract 91-1211A.

References

[1] Van Den Braembussche R.A., Calculation of Compressible Subsonic Flow in Cascade with Varying Blade Height, *ASME J. of Eng. Power* **95** (1973) 345-351.

[2] Martensen E., Die Berechnung der druckverteilung an dicken gitterprofilen mit hilfe von Fredholmschen Interglagleichungen, *Arch. Rat. Mech. Anal.* **3** (1959) 235-270.

[3] Chauvin J., Yazigi N., Charlier M.H. and Gerolymos G.A., Performance Prediction of Subsonic Separated Cascades (1990), ASME paper N° 90-GT-65.

[4] Schlichting H., Boundary Layer Theory (McGraw-Hill Book Company, 7th Edition, 1979).

[5] Papailiou K.D., Optimisation d'aubage de compresseur à forte charge sur la base des théories de couches limites, Doctoral Dissertation, Université de Liège (Liège, Belgique, 1969).

[6] Huo S., Optimisation Based on The Boundary Layer Concept For Compressible Decelerating Flows, Ph. D. Thesis, VKI - Institut Aéronautique ULB (Belgium, Octobre 1973).

[7] Lefoll, A theory of Representation of the Boundary Layer Properties on a plane, Paper, Seminar on Advanced Problems in Turbomachinery (Brussels, Belgium, 1965).

[8] Papailiou K.D., Optimisation des dispositifs décélérateurs à forte charge basée sur une théorie intégrale de la couche limite, Doctoral Dissertation, Université Claude Bernard (Lyon, France, 1974) pp. 50-60.

[9] Coles D.A., The Law of the Wake in the Turbulent Boundary Layer, *J. Fluid Mech.* **1** (1956) 191-226.

[10] Jacob K., Berechnung der abgelösten inkompressiblen strömung um tragflügelprofile und bestimung des maximalen auftriebs, *Z. Flugwiss* **15** (1969) 357-367.

[11] Janssens P. and Hirsch Ch., A viscid and inviscid interaction procedure for two dimensional cascades, AGARD CP 351, Denmark (June 1983) pp. 3-1, 3-18.

[12] Geller W., Incompressible Flow Through Cascades with Separation, In "Boundary Layer Effects in Turbomachines", AGARD AG 164. (Dec. 1972) 175-186.

[13] Van Den Braembussche R.A., Modèle Non-Visqueux de Poche de Décollement, Private Communications (1988).

[14] Goujon-Dubois A., Calcul d'un écoulement incompressible décollé dans une grille d'aubes, Mémoire de fin d'Etudes, Université de Liège et V.K.I. de Dynamique de Fluides (1972).

[15] Jacob K., Computation of the Flow Around Wings with Rear Separation, DFVLR-Bericht FB 82-22 (1982).

[16] Morkovin M.V., On the Many Faces of Transition, Viscous Drag Reduction. C.S. Wells Ed. (Plenum Press, New York 1969) pp. 1-31.

[17] Mayle R.E. and Dullenkopf K., A Theory for Wake-Induced Transition, *ASME J. of Turbomachinery* (ASME Paper 89-GT-57) **112** (1990) 188-195.

[18] Emmons H.W., The Laminar-Turbulent Transition in a Boundary Layer-Part 1, *J. Aero. Sci.* **18** (1951) 490-498.

[19] Michel R., Aérodynamique-Couches Limites, Frottement et Transfert de Chaleur (ENSAE Editions, Toulouse, 1972) pp. 10-6, 10-25, also see ONERA Publications N° 58, 1952.

[20] Abu-Ghannam B.J. and Shaw R., Natural Transition of Boundary Layers-The Effects of Turbulence, Pressure Gradient and Flow History, *J. Mech. Eng. Sci.* **22** (1980) 213-228.

[21] Van Driest E.R. and Blumer C.B., Boundary Layer Transition: Free Stream Turbulence and Pressure Gradient Effects, *AIAA J.* **1** (1963) 1303-1306.

[22] Cousteix J., Turbulence et Couche Limite, Cepadues Ed. (Toulouse 1989).

[23] Arnal D., Habiballah M. and Coustols E., Théorie de L'Instabilité Laminaire et Critères de Transition en Ecoulement Bi- et Tridimensionnel, *La Recherche Aérospatiale* (1984) 125-143.

[24] Arnal D., Habiballah M. and Delcourt V., Synthèse sur les Méthodes de Calcul de la Transition Développées au DERAT, ONERA CERT Rapport Technique OA N° 11/5018 AYD (Juin 1980).

[25] Dhawan S. and Narasimha R., Some Properties of Boundary Layer Flow During Transition from Laminar to Turbulent Motion, *J. Fluid. Mech.* **3** (1958) 418-436.

[26] Mayle R.E. and Dullenkopf K., More on the Turbulent-Strip Theory for Wake-Induced Transition, *ASME J. of Turbomachinery* (ASME Paper 90-GT-137) **113** (1991) 428-432.

[27] Kus U. and Chauvin J., A Rapid Method for Predicting Global and Local Performance of Cascades with Special Emphasis on the Calculation of the Transition Region, *ASME* Paper 94-GT-256 (1994).

[28] Gostelow J.P., Blunden A.R. and Walker G.J., Effects of Free-Stream Turbulence and Adverse Pressure Gradients on Boundary Layer Transition, *ASME* paper 92-GT-380 (1992).

[29] Walker G.J., Transitional Flow on Axial Turbomachine Blading, *AIAA J.* **27** (1989) 595-602.

[30] Walker G.J. and Gostelow J.P., Effects of Adverse Pressure Gradients on the Nature and Length of Boundary Layer Transition, *ASME J. Turbomachinery* **112** (1990) 196-205.

[31] Roberts W.B., A Study of the Effect of Reynolds Number and Laminar Separation Bubbles on the Flow through Axial Compressor Cascades, Doctoral Dissertation, Université Libre (Brussels, Belgium, 1973).

[32] Roberts W.B., A Study of the Effect of Reynolds Number and Laminar Separation Bubbles on the Flow through Axial Compressor Cascades, *ASME J. Eng. Power* **97** (1975) 261-274.

[33] Roberts W.B., Calculation of Laminar Separation Bubbles and their Effect on Airfoil Performance, *AIAA J.* **18** (1980) 25-31.

[34] Horton H.P., Laminar Separation Bubbles in 2D and 3D incompressible Flow, Doctoral dissertation, University of London (London, U.K., 1968).

[35] Hodson H.P., Boundary Layer and Loss Measurements on the Rotor of an Axial-Flow Turbine, *ASME J. Eng. Gas Turbines Power* **106** (1984) 391-399.

[36] Pfeil H., Herbst R., Transition Procedure of Instationary Boundary Layers, *ASME* Paper 79-GT-128 (1979).

[37] Pfeil H., Herbst R. and Schröder T., Investigation of the Laminar-Turbulent Transition of Boundary Layers Disturbed by Wakes, *ASME J. Eng. Power* **105** (1983) 130-137.

[38] Hodson H.P., Addison J.S. and Shepherdson C.A., Models for Unsteady Wake Induced Transition in Axial Turbomachines, *J. Phys. III France* **2** (1992) 545-574.

[39] Obremski H.J. and Fejer A.A., Transition and Oscillating Boundary Layer Flow, *J. Fluid Mech.* **29** (1967) 93-111.

[40] Schubauer G.B. and Skramstad H.K., Laminar Boundary Layer Oscillations and Transition on a Flat Plate, NACA Rept. 909 (1948).

[41] Hodson H.P., Modelling Unsteady Transition and Its Effects on Profile Loss, Proc. AGARD Conf. PEP 74 a, On Unsteady Flows in Turbomachines, AGARD-CP-468.

[42] Gostelow J.P. and Walker G.J., Similarity Behaviour in Transitional Boundary Layers over a Range of Adverse Pressure Gradients and Turbulence Levels, *ASME J. of Turbomachinery* (ASME paper 90-GT-130) **113** (1991) 617-625.

[43] Mayle R.E., The Role of Laminar-Turbulent Transition in Gas Turbine Engines, *ASME J. of Turbomachinery* (ASME Paper 91-GT-261) **113** (1991) 509-537.

[44] Simpson R.L., Two Dimensional Turbulent Separated Flow, *AIAA J.* **25** (1987) 775-777.

[45] Heilmann W., The Influence of Axial Velocity Density Ratio On Compressor Cascade Performance in Compressible Flow, AGARD-AG-164, Boundary Layer Effects in Turbomachines (December 1962).

[46] Yazigi N., Modélisation des écoulements bidimensionnels stationnaires incompressibles en grilles d'aubes décollées, Thèse de Doctorat de l'Université Pierre et Marie Curie (Paris, France, Octobre 1992).

[47] Herrig L.J., Emery C.J. and Erwin R.J., Systematic Two-Dimensional Cascade Tests of NACA 65-Series compressor Blades at Low Speeds, NACA TN 3916, Langley Aeronautical Laboratory (Washington, February 1957).

[48] Dunavant C.J. and Erwin R.J., Investigation of a Related Series of Turbine-Blade Profiles in Cascade, NACA TN 3802, Langley Aeronautical Laboratory, Washington (October 1956).

[49] Deutsch S. and Zierke W.C., The Measurement of Boundary Layers on a Compressor Blade in Cascade - Part 1: A unique Experimental Facility, *ASME J. of Turbomachinery* (ASME Paper N°87-GT-248) **109** (1987) 520-526.

[50] Deutsch S. and Zierke W.C., The Measurement of Boundary Layers on a Compressor Blade in Cascade - Part 2: Suction Surface Boundary Layers, *ASME J. of Turbomachinery* (ASME Paper N°87-GT-249) **110** (1988) 138-145.

[51] Deutsch S. and Zierke W.C., The Measurement of Boundary Layers on a Compressor Blade in Cascade - Part 3: Pressure Surface Boundary Layers and the Near Wake, *ASME J. of Turbomachinery* (ASME Paper N°: 87-GT-250) **110** (1988) 146-152.

[52] Deutsch S. and Zierke W.C., The Measurement of Boundary Layers on a Compressor Blade in Cascade - Part 4: Flow Fields for Incidence Angles of −1.5 and −8.5 Degrees, *ASME J. of Turbomachinery* (ASME Paper N°: 89-GT-72) **112** (1990) 241-255.